Design and Evaluation of 'BTTN' – A Backscattering Tag-to-Tag Network

Jihoon Ryoo, Jinghui Jian, Akshay Athalye and Samir R. Das
Stony Brook University
Stony Brook, New York, USA

ABSTRACT

RF-powered backscatter communication between passive tags holds tremendous potential for ubiquitous deployment of 'Internet of Things' (IoT). We develop BTTN, a *Backscattering Tag-to-Tag Network* platform, that communicates via backscatter modulation of an external RF excitation signal. This set up gives rise to a unique phase cancellation problem which gravely limits the range and reliability of such tag-to-tags link. We develop a novel multi-phase backscatter modulation technique with a learning mechanism that overcomes this problem efficiently. This improves the link performance bringing passive tag-to-tag communication closer to practical use. We develop prototype BTTN tag hardware and firmware and evaluate its performance. The prototype achieves link ranges of up to 3 m at 5 Kbps with an excitation power level of only -20 dBm while successfully overcoming phase cancellation. We further extend BTTN operation to a multihop network where we demonstrate a 4 hop link capable of communicating over 12 m under similar conditions. Higher power provides longer ranges. BTTN provides competitive or better link performance with respect to existing work while using far less complex techniques.

1. INTRODUCTION

Practical technologies for 'Internet of Things' (IoT) must be able to provide connectivity to all objects under a common framework irrespective of their size or value. Power requirement, cost of wireless devices and scalability has proved critical bottlenecks for universal deployment of the IoT. The standard approach of combining low-power micro-controller/CPU and RF transceivers for IoT is considered too power hungry – mainly due to the use of an active on-board radio transceiver. The leanest of the commodity radio transceivers catering to the embedded RF devices market consumes in the order of mW even when idle (listening) and in the order of tens of mW when actively transmitting or receiving. This is at least two orders of magnitude higher than the power consumed by commodity low-power microcontrollers in equivalent states (CPU idle and CPU active states). Moreover, use of active radios increases the cost of the devices and also invariably necessitates the use of on board batteries which add a significant management overhead.

Potential of Backscatter Communications.

One approach to eliminating the power hungry active radio from the system is the use of a communication paradigm where devices communicate via *backscattering* and exploit harvested power from an external RF source. This brings down the size, power, and cost of an IoT platform to an unprecedented level. Backscattering works by modulating an RF signal (transmitted from an external source) incident on the antenna of the device. The modulation is achieved simply by changing impedance levels seen by the antenna of the platform, thereby changing its reflection coefficient. The minimal intelligence needed to achieve this requires very little power. If designed correctly, the power supplied by the external RF signal itself is sufficient to drive the device electronics. Today, the most widely used embodiment of this technology is in RFID (Radio Frequency IDentification) [17, 19]. In RFID this simple device is known as the 'tag' and the external RF signal is provided via a relatively higher power embedded computer, possessing an active radio, called the 'reader.' The reader also receives and interprets the modulated signal backscattered by the tag and provides specific instructions to the tag about how to respond. But this reader-based system, while widely used, suffers from a serious scalability issue: tags can only talk to readers and not to themselves. Thus, there must be enough readers to 'cover' all the tags in an environment. Further, the readers themselves need to be networked and centrally controlled. These factors severely deter the practical viability of a large-scale IoT based on traditional RFID technology.

Tag-to-Tag Backscatter.

The general goal of our work is to extend backscattering to its logical extreme so that conventional readers are no longer required. We create a *Backscattering Tag-to-Tag Network* or *BTTN* (pronounced 'button') wherein backscattering tags are themselves able to read and interpret the backscattered communications from

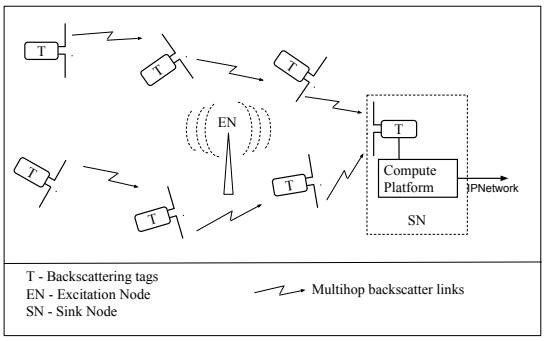

Figure 1: Proposed BTTN tag network.

other neighboring tags, thus producing a multihop network of tags. A gateway or sink node can connect this network to an external IP network as needed. We design and build the constituent tags of BTTN that we refer to as 'BTTN tags.' The initial feasibility of this form of tag-to-tag communication has been demonstrated by our prior work [11, 12, 13] as well as by others [29, 26]. But these studies fall short of demonstrating a multihop relaying operation. BTTN also overcomes a unique phase cancellation phenomenon that occurs in all backscattering tag-to-tag links that these prior works did not address.

BTTN tags indeed require external RF sources (we call them 'exciters') for powering and backscattering (see Figure 1). However, the exciters here simply feed RF power and have zero intelligence. Unlike standard RFID readers, these external sources could be much fewer in number as there is no reverse link under consideration. With no intelligence, they are of very low cost and can be simply integrated into the infrastructure of the future as a standard practice.

Using Ambient RF Signals for Excitation.

Ambient RF signals (e.g., TV or WiFi signals) can also serve the purpose of exciters [26, 15]. In this case, TV towers or wireless transmitters take up the role of the exciters. However, designs solely based on such ambient signals may be too restrictive, as not all environments may have the required signal power levels. For example, in [26] tag-to-tag communication has been studied with ambient TV signal powers between -24 dBm and -8 dBm. This level of TV power available indoor is quite unusual.[1] Similar issues exist with backscattering with ambient WiFi signals as well [24, 15]. In BTTN, we assume that the exciter can either be a naturally present, suitable RF source in the environment or a deliberately deployed device. In our work we experiment both with continuous wave (CW) signals as well as DTV signals produced by a software radio in the 900 MHZ ISM band.

Contributions.

In the absence of an active transceiver, BTTN tags use passive envelope detection techniques [17] to demodulate backscatter signals from neighboring tags. However, this approach comes with a problem. On the receiving tag the excitation signal and the backscattered signal superimpose at different phases depending on the tag location. The relative phase difference between the two signals at the receiving tag impacts the baseband signal envelope. This phenomenon causes the detected signal to be severely attenuated and even completely canceled out even when two tags may be in the 'vicinity' of each other in terms of backscatter signal strength. In a prior work we have mathematically analyzed this phenomenon [31]. This happens regardless of whether the excitation signal is a CW signal or an ambient signal such as TV signal. We address this problem by employing phase diversity at the backscattering tag whereby the tag has the ability to backscatter in multiple *phase channels* each differently altering the phase of the backscattered signal. This simple mechanism improves link performance significantly while introducing only minimal hardware complexity.

The contributions of this work are summarized as follows:

1. We demonstrate that by employing our phase diverse backscattering scheme one can overcome the phase cancellation problem and form tag-to-tag links up to about 3 m at 5 Kbps when the available excitation power is about -20 dBm. We get a significantly better range (up to about 10 m though with some gaps) when the power increases to about -15 dBm. This is competitive or better relative to recent work [26, 30] if one considers combination of all three factors – distance, available power and bit rate, while using a much simpler technique.

2. We use a simple learning mechanism to determine the right phase channel to use for each link. Using this mechanism we demonstrate multihop operation for upto 4 hops, thus enabling tag-to-tag communication over about 12 m at 5 Kbps with only -20 dBm available excitation power.

The rest of the paper is organized as follows. In Section 2 we describe the overall design of the BTTN tags.

[1] For example, in [14] the authors report a maximum power level of -65 dBm at building rooftops and much less in building interiors in Turin, Italy. In vehicular measurements outdoors in Madison, Wisconsin, the authors in [34] report a maximum power level of about -50 dBm that too when closer than 1 km from a TV tower. Our own experience in measurement campaigns in New York metro areas [16] is also generally in line with these measurements.

Here, we describe and address the phase cancellation problem. In Section 3 we present the BTTN prototype and evaluate a single link performance. In Section 4 we describe and evaluate the multihop operation. We describe related work in Section 5 and conclude in Section 6.

2. BTTN TAG DESIGN

As shown in Figure 2, a BTTN tag consists of an antenna, a receive (Rx) or demodulation section, data processing & transmit (Tx) section and a power management section.

2.1 Antenna and Receive Sections

Antenna Section.

To achieve omnidirectional communication on horizontal plane, a dipole-style antenna with its donut-shape radiation pattern is a good choice for the BTTN tag. The dipole is also a good choice for ubiquitous tagging since it is low cost and easy to manufacture in printed and wire form. A lumped LC balun is deployed at the antenna port for connection to the tag RF section to achieve better matching and radiation.

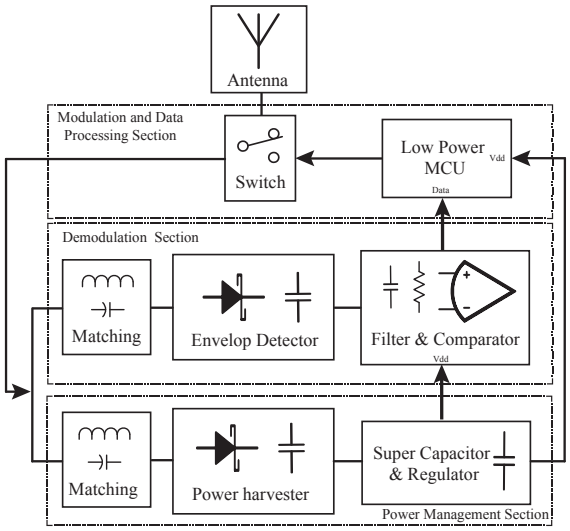

Figure 2: Schematic of various modules in a BTTN tag

Receive Section.

The Receive (Rx) section consists of a matching circuit designed to maximize power transfer, an envelope detector, an RC filter to cut off unwanted frequencies, leaving only baseband signal, and a comparator to digitize the analog signal. At the input of the detector we employ a "T"-shaped narrow-band matching network made of three lumped devices which match the detector to 50 Ω at 915 MHz. This is right at the middle of the 902-928 MHz band we have chosen for the design and evaluation of BTTN. The excitation for our network is provided by a radio signal generator operating in this range (see Section 3.1). The design principles and the findings are equally applicable to systems which utilize excitation signals at different frequencies. To use our tags at other frequencies, the only changes needed will be in the dimensions of the dipole antenna and the values of the lumped components used in the matching network.

In a BTTN link, the transmitting tag backscatters a fraction of the external excitation signal. As a result, the backscatter signal at the receiving tag has inherently low signal strength and is superimposed with the stronger external excitation signal. Hence the Rx section sees a signal with a very low effective modulation depth and requires a highly sensitive detector to demodulate this signal. We use an envelope detector with a 4-stage voltage multiplier to boost up the received baseband signal and effectively extend the tag-to-tag range. The schematic of the detector is shown in Figure 3, in which the voltage multiplier is realized by combination of Schottky diodes ($D_1 - D_4$) and capacitors ($C_1 - C_4$). We use the HSMS-285x series, zero-bias Schottky diodes from Avago Technologies [4] for our implementation. The capacitor in the last stage C_4 and a load resistor R_1 form the RC filter to cut off the excitation RF signal, leaving only the baseband; the parameters of the RC filter are tuned to produce a clean baseband signal.

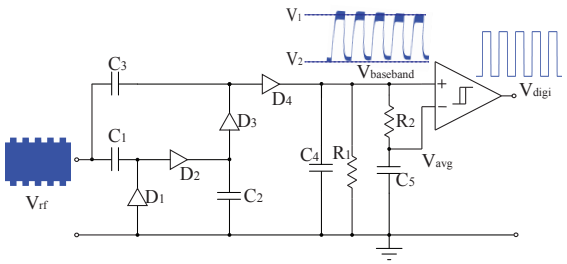

Figure 3: Schematic of passive envelop detector in BTTN

There are tradeoffs involved in the selection of component values. For instance, using a large R_1 can increase the output voltage, but this also limits the data rate of the baseband signal. At the same time, decreasing C_4 can mitigate this problem at the cost of increasing ripple amplitude. Considering these factors, we use $R_1 = 100$ kΩ and $C_4 = 20$pF. This allows for baseband signal frequencies of up to 20kHz without signal distortion or noise corruption. A second RC filter implemented by R_2 and C_5 with a large time constant is used to generate an average reference voltage V_{avg} for the comparator. The cutoff frequency of this filter also affects the bandwidth of the entire detector. Finally, a comparator with internal hysteresis is used as 1-bit ADC to digitize the detected baseband sig-

nal (V_{baseband}). The output of the comparator (V_{digi} is fed to a low-power microcontroller (MCU) for decoding. The encoding and decoding schemes are outlined later in Section 2.5. We use the Texas Instrument's MSP430 [7] as the MCU for our prototype tag.

2.2 Phase Cancellation Problem

A BTTN transmitting tag achieves backscattering by altering the terminating impedance of its antenna between two states 1 and 2. Two different backscattering techniques can be used:

1. Amplitude Shift Keying (ASK) backscatter wherein the *real* part of the tag impedance is altered in the two states. This causes a variation in the amplitude of the backscattered signal,
2. Phase Shift Keying (PSK) Backscatter wherein the *imaginary* part of the tag impedance is altered in the two states. This causes a variation in the phase of the backscattered signal.

In the BTTN receiver, the backscatter signal from the transmitting tag is superimposed with the external excitation signal. In an ideal case, i.e. if the two signals are in phase, the pattern of this combined signal is similar to V_{rf} as shown in Figure 3. Assume that the output voltage of the detector in the two states is V_1 and V_2 respectively (Figure 3). Then the voltage difference $|V_1 - V_2|$ corresponds to the amplitude of the received backscatter signal. However in practice, the excitation signal and the received backscatter signal may not be in phase, but have a relative phase difference which is a function of the received power levels and the relative positions of the tags and the exciter. The combination of the two signals at the input of the passive detector causes a unique phase cancellation problem that profoundly impacts the tag-to-tag link. We demonstrate this phenomenon with the help of phasor diagrams that show the combined electric fields in terms of their respective amplitudes and phases.

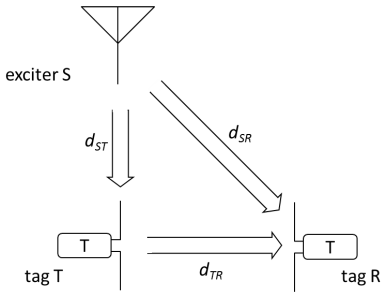

Figure 4: A BTTN link between two tags also showing the exciter.

Consider a simple BTTN setup as shown in Figure 4 consisting of one excitation source, S, and two tags, viz. a transmitting tag T and receiving tag R. The respective distances between three devices are shown in the figure. In such a setup, there are 3 electric fields, viz. the excitation field at T from S, denoted by $\mathbf{E}_{T,S}$, the excitation field at R from S, denoted by $\mathbf{E}_{R,S}$, and the backscatter modulated field at R from T, denoted by $\mathbf{E}^i_{R,T}$, with i = 1,2 representing the two backscatter modulation states.

The excitation field at R is determined by

$$\mathbf{E}_{R,S} = I_{\text{S}}\sqrt{\frac{\eta G_{\text{S}} R_{\text{S}}}{4\pi d^2_{\text{SR}}}} e^{-j(\beta d_{\text{SR}} + \frac{\pi}{2})} \tag{1}$$

where I_{S} is driving current in the exciter, η is the medium impedance which is 377 Ω for free space and air, β is the propagation constant given by $2\pi/\lambda$, and G_S and R_S are the gain and resistance of the exciter antenna. The incident exciter field at the transmit tag $\mathbf{E}_{T,S}$ can also be calculated using the above equation. This field in equation 1 can be written in terms of its amplitude and phase as:

$$\mathbf{E}_{R,S} = A_{R,S} \cdot e^{j\theta_{R,S}}, \tag{2}$$

where $A_{R,S}$ is the amplitude and $\theta_{R,S}$ is the phase of the field. The other fields mentioned above can also expressed similarly in terms of their amplitude and phase. The amount of the incident excitation field backscattered by the transmit tag is determined by its complex reflection coefficient, Γ^{*i} which is in turn determined by the impedance connected to the tag antenna. This impedance is altered between 2 states i = 1,2 to achieve the modulation. Thus, the total resultant field received at tag R for each modulation state can be written as:

$$\mathbf{E}^i_{\text{R}} = \left(\mathbf{E}_{R,S} + \mathbf{E}^i_{\text{R,T}}\right) = \left(\mathbf{E}_{R,S} + \Gamma^{*i} \cdot \mathbf{E}_{T,S}\right) \tag{3}$$

$$= A^i_{\text{R}} e^{j\theta^i_{\text{R}}} \qquad \text{i} = 1, 2. \tag{4}$$

For this analysis, we assume that the tag employs ASK backscattering, i.e. the amplitude of the backscattered signal in the two states changes, but the phase remains the same (i.e. $\theta^1_{R,T} = \theta^2_{R,T}$). This is also consistent with what our prototype BTTN platform implements.

We demonstrate the field interactions using the phasor diagrams in Figures 5. To simplify these phasors, we consider the phase of the field $\mathbf{E}_{R,S}$ (i.e. $\theta_{R,S}$) to be the reference phase and plot the phase of the other signals relative to his. We have presented a more detailed mathematical and phasor analysis of this phenomenon in [31, 22]. Figure 5(a) shows the phasor diagram in a situation where phase cancellation does not happen. The phase difference θ between the superimposing signals is such that amplitude of the resultant signals in the two states are different. In this case the amplitude of the signal at the output of the detector is nonzero ($|V_1 - V_2|$) and the backscatter signal is detected. However, in the scenario shown in Figure 5(b), the superimposing signals line up in such a way that the amplitudes

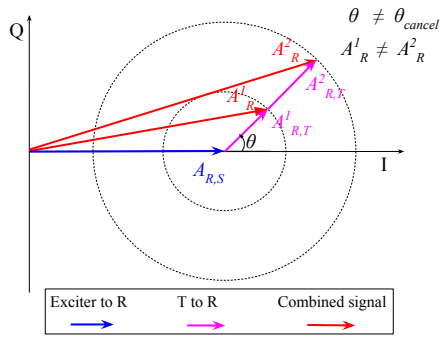

(a)Cancellation does not occur

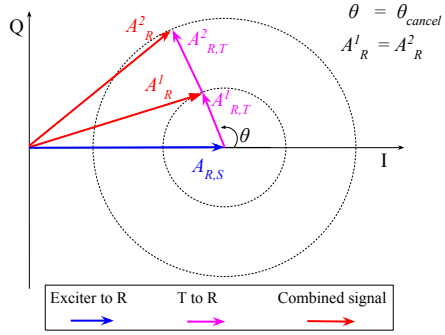

(b) Cancellation occurs

Figure 5: Phasor diagram showing received signal when cancellation (a) does not occur or (b) occurs

of the resultant signals in the two modulation states are the same. In this case, the detected voltages in the two states are the same ($V_1 = V_2$) and the backscatter signal is canceled out at the receiving tag.

The reader may wonder whether this form of phase cancellation is limited to only very specific locations. Our analysis in [31, 22] has shown that this is pervasive. Even when there is no complete cancellation, the amplitude of the detected backscatter signal ($|V_1 - V_2|$) could be too small for the comparator to digitize the bits accurately. Figure 6 shows this amplitude with increasing tag-to-tag distance for a fixed position of the exciter. This plot is obtained via analytic modeling not shown here for brevity.

As seen from the figure, in the absence of phase cancellation (i.e. in the absence of excitation signal superimposing with the backscatter), the amplitude of the received backscatter will decrease monotonically with increasing tag-to-tag distance (blue line). However, because of phase cancellation, the amplitude does not vary this way, but rather varies continuously between peaks and nulls with successively decreasing peaks (red line). This figure shows that the impact of the phase problem on the tag-to-tag link is much more severe than that a handful of randomly occurring null points. In fact, other than a few points (where the two lines in Figure 6

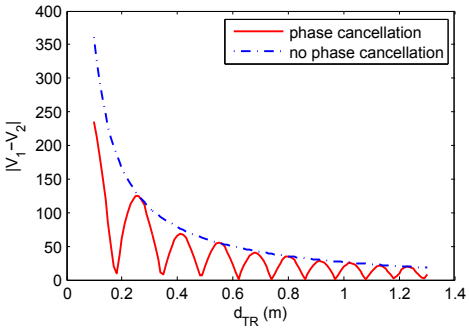

Figure 6: Received voltage difference $|V_1 - V_2|$ with and without consideration of phase cancellation (obtained via analytical modeling

intersect) the received backscatter is always attenuated due to this phenomenon.

2.3 Multi-Phase Backscatter

One potential mechanism to address the phase cancellation problem is to employ multiple antennas on the tag to obtain some form of phase diversity [33, 24]. This solution has the downside of making the tag bigger in size and bulky. The approach also has limited scalability, since to obtain more phase diversity, one would have to add more antenna elements making the tag even bulkier. In addition, the difference between the relative phases of overlapping signals at the multiple antennas is not deterministic and is affected by environmental geometry and inter-tag distance. Also for BTTN systems utilizing excitation signals at lower frequencies (e.g., 433 MHZ), the distance between the antennas need to be even longer to get enough phase diversity.

Instead, we propose a solution wherein phase diversity is introduced in the backscatter modulator of the transmitting tag. This is done by using a multi-port backscatter modulator that provides the BTTN tag the ability to backscatter in one of several *phase channels*.[2] Each channel is characterized by a different reflection coefficient, and adjacent channels are separated by a *fixed and deterministic* phase difference. The basic idea is to have the ability to transmit a message over multiple phase channels available on the tag. Then, at the receiving tag, even if the message is canceled or severely attenuated in one channel, it will still be detected in another channel. For example, looking at Figure 5, the subfigures (a) and (b) illustrate how two possible phase channels might work.

Exploiting this form of phase diversity at the transmit side have several advantages over competitive multi-antenna approaches:

[2]The term 'channel' is used here in the abstract to signify a different transmission mode that causes a phase shift relative to other modes and not a different frequency band.

1. The phase channels are implemented simply by using additional passive components (resistors and capacitors). As a result it is easier to implement and has negligible impact on the size of the tag.
2. There will always be a fixed, deterministic phase difference between the backscatter signals in the different channels at the receiver. This is irrespective of the setup geometry or inter-tag distance because these factors affect all channels equally. Hence, this approach provides a deterministic solution to the problem that is not influenced environmental randomness.
3. This approach is very scalable since the number of phase channels can be increased by adding more passive RC components without increasing the complexity of the tag significantly. In fact, extending this concept to its logical extreme, with a large enough number of phase channels on the backscatter modulator, the tag-to-tag link can approach ideal performance indicated by the blue line in Figure 6 i.e. completely nullify the effect of phase cancellation.

Obviously, under a straightforward, brute force implementation of this approach, whereby a tag transmits the same message repeatedly over all available phase channels, the throughput of the network will be greatly reduced. BTTN employs a simple learning mechanism that learns that best channel to use via simple probing. We discuss more on this in Section 4.1.

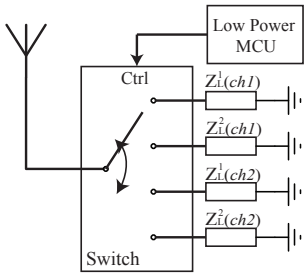

Figure 7: Implementation of multiphase backscatter modulator using an RF switch controlled by the MCU

Implementation.

The implementation of our multiphase backscatter modulator is shown in Figure 7. Choosing the appropriate values for the reflection coefficient and hence the load impedances for the different phase channels is an important step in the implementation of the proposed scheme. Let $\Delta\Gamma^*(ch1)$ and $\Delta\Gamma^*(ch2)$ be the difference between the two modulation states of the complex reflection coefficient for channel 1 and 2 respectively (i.e. $\Delta\Gamma^* = \Delta\Gamma^{*1} - \Delta\Gamma^{*2}$). Then, in order to realize the technique described above, we need to satisfy the following condition:

$$\Delta\Gamma^*(ch2) = \Delta\Gamma^*(ch1) \cdot e^{j\theta_d}, \tag{5}$$

where θ_d is the effective phase difference between the signals backscattered in the two channels. According to our analysis in [22], to obtain the largest amplitude differences in one channel when the other faces phase cancellation, the best value for θ_d is $\pi/2$. Now we can map Γ^* to the Smith Chart to get the values of the impedances needed for the two channel. To make the mapping more convenient, we use power reflection coefficient γ defined by Kurokawa in [25, 28]:

$$\gamma^i = \frac{Z_L^i - Z_A^*}{Z_L^i + Z_A}, \mathrm{i} = 1, 2, \tag{6}$$

where Z_A is the tag antenna impedance and Z_L^i is the load impedance provided by the backscatter modulator in modulation state i, $\Gamma^* = -\gamma$, and $\Delta\Gamma^* = -\Delta\gamma$.

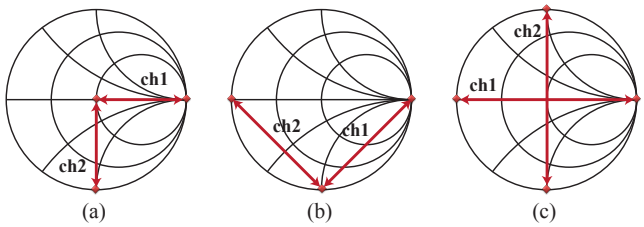

Figure 8: Three modulation schemes for two phase channels on normalized Smith charts in term of γ

Figure 8 shows three possible modulation schemes for two phase channels on normalized Smith charts in term of γ_L. One important factor to note is that the choice of reflection coefficient affects the instantaneous power that can be harvested from the incident field. From the figure, it is obvious that modulation scheme(a) maximizes the backscatter signal strength by maximizing $\Delta\gamma$. However, this can also cause a big drop in the instantaneous harvested power for the duration of a bit period during backscattering. This also requires inductive components as part of the backscatter modulator. Alternatively, scheme(b) can produce $\theta_d = \pi/2$ using only RC components. Scheme(c) implements the phase channels without any loss of instantaneous harvested power at the cost of reduced backscatter strength. The $\Delta\gamma$ for three modulation schemes is shown in Table 1 as well as corresponding γ^i. After locating the reflection coefficients for the various phase channels on the Smith Chart, the required impedance values to implement these channels are easily calculated.

Our prototype tag implements scheme(a) for the multiphase backscattering. Using an antenna characteristic impedance of $Z_A = 50\Omega$, and the methodology described above, the load impedances for the phase channels are calculated to be $Z_{\mathrm{L},2}^{\mathrm{ch1}} = \infty$ (open circuit), $Z_{\mathrm{L},2}^{\mathrm{ch2}}$

Table 1: $\Delta\gamma$ for the 3 modulation schemes considered

	Channel 1			Channel 2		
	$\Delta\gamma_L$	γ_L^1	γ_L^2	$\Delta\gamma_L$	γ_L^1	γ_L^2
scheme (a)	$1e^{j0}$	0	1	$1e^{-j\frac{\pi}{2}}$	0	-j
scheme (b)	$\sqrt{2}e^{j\frac{\pi}{4}}$	-j	1	$\sqrt{2}e^{j\frac{3\pi}{4}}$	-j	-1
scheme (c)	$2e^{j0}$	-1	1	$2e^{j\frac{\pi}{2}}$	-j	j

$= -j50$ ($C \approx 3.6$ pF for 915 MHz), and $Z_{L,1}^{ch1} = Z_{L,1}^{ch2} = 50\Omega$, which is realized by matched detector. We have used a CMOS FET switch (ADG904 from Analog Devices) for the RF switch used in the backscatter modulator.

2.4 Evaluation of Power Consumption

The BTTN tag prototype has 3 active components that contribute to the power consumption, viz. the RF switch operating as the backscatter modulator, the comparator and the MCU. In our implementation, the switch used is the ADG 904 from Agilent Technologies [9], the comparator is the MCP6561 from Microchip Technologies [6] and the MCU is the MSP 430 from Texas Instruments [7]. We have evaluated the power consumption of each active part by measuring the current in each of these devices during the different modes of operation (Tx, Rx) with a power supply of 2V. The current is measured using the 34401A digital multimeter from Keysight. We measure the total current through the digital part (MCU) as well as the total current through the analog part (switch and comparator).

The ADG 904 switch has a quiescent DC current 100 nA or a quiescent power consumption of 0.2 μW. The dynamic power consumption of the switch during data transmission is a function of the data rate. It can be calculated as $1/2CV^2f$ where C is the capacitance at the switch input, V is the supply voltage and f is the data rate [32]. Based on this information and the total current measured through the analog part of the device, we can determine the current consumed individually by the switch and the comparator. The comparator MCP6561 is chosen for our prototype because it can support higher input frequencies of 1 MHz or higher, and its power consumption does not go up significantly for input frequencies below 100 KHz [6]. This makes our prototype flexible enough to handle a wide range of bit rates. Another option would have been to use the TS8811 as in [26]. This comparator has a much lower current consumption (around 700 nA). But the propagation delay is 30 to 40 times larger which means that higher input frequencies cannot be supported. Generally speaking, the comparator is active only in the receive/sensing mode and the switch is active only in the transmit mode.

Table 2: Power consumption in the 3 active components in BTTN tags

	Tx		Rx	
	$I(\mu A)$	$P(\mu W)$	$I(\mu A)$	$P(\mu W)$
Comparator	70	140	71	142
Switch	0.14	0.28	0.1	0.2
Microcontroller	60.5	121	204	408

The power consumption of all active devices is summarized in Table 2. The digital section dominates the power consumption. It is important to note that the power consumption values measured above (particularly in the case of the digital section) are higher on account of the use of discrete components used to build the BTTN tag prototype. It is expected that it practice such a tag will be manufactured as a single chip using established ASIC design procedures. This will significantly reduce the power consumption and the cost of the BTTN tag.

As a final note, it is instructive to compare the power consumption of BTTN with other recent related designs [26, 30]. Discounting the MCU power, the power consumption in [26] and in the μcode design in [30] are lower ($< 1\mu$W and $< 10\mu$W respectively). But they also provide lower data rates or lower ranges when similar excitation power levels are considered at the backscaterring tag. This is primarily due to the use of a lower power comparator which also limits the data rate as explained above. In the μmo design in [30], the power consumption is higher ($> 400\mu$W), but it is able to perform at a higher data rate (1Mbps) though only at limited ranges. We also point out that compared to these designs, the BTTN tag incorporates the multi-phase backscattering mechanism which greatly enhances link performance without adding significantly to the power consumption.

2.5 Physical Layer Design

In this section, we describe various physical layer characteristics of our BTTN tags.

Encoding.

Because of the passive modulation and demodulation techniques employed in BTTN tags, delay (or transition) encoding mechanisms like Miller and FM0 are a good fit. In such schemes the data to be transmitted is represented by the presence or absence of high-low transitions at the boundaries or the center of a symbol. These encoding schemes have been widely researched in the context of standard RFID systems [8]. We use Miller modulated subcarrier encoding with multiplication factor M-2 (Miller-2 encoding). This provides a good data rate vs noise immunity tradeoff. Also this encoding can be easily scaled up to Miller-4 or Miller-8 to further increase noise protection at the cost of data

rate. Our BTTN tags have used an on-board clock of 10 KHz and a link data rate of 5 Kbps.

Pilot Tone.

The pilot tone is simply a sequence of identical symbols. In traditional RFID, it helps the reader to identify the start of a tag packet. In the BTTN tag however, it is serves a more important functions. The BTTN tag receiver is a passive envelope detector followed by a comparator. As explained in Section 2, the threshold value of this comparator is dynamically set to the average of the detector output. The presence of the pilot tone allows the RC circuit producing this reference voltage to charge up to the required threshold value well before the actual preamble bits arrive. This ensures that when the actual data bits arrive, the comparator threshold is set to the proper value for correct digitization.

When the pilot tone is used in the Tx packet, the MCU can be put into a low power idle mode while listening. Then the pilot tone serves to issue an interrupt to the MCU that forces it into a preamble detection mode. The length of the tone gives the MCU enough time to complete this transition and process the preamble bits without any loss. This mechanism saves about 200μA in current consumption at the MCU. We use a sequence of ten 0's encoded using the Miller-2 scheme as our pilot tone.

Decoding.

Decoding is implemented on the BTTN MCU by sampling the output of the comparator and measuring the time between edge transitions. This time between successive transitions is mapped to the decoded data bits. For the decoder the pilot tone can provide calibration to compensate for clock drifts or other timing drifts in the MCU. Timing of the edge transitions in the pilot tone at the start of each packet is used as a reference to decode bits in the remainder of the packet. Clearly a higher input sampling rate with add robustness to the decoder. But this would require a higher clock speed which can add to the power consumption. Our chosen data rate of 5 kbps provides a good balance between noise immunity and power consumption.

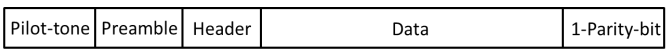

Figure 9: Packet format in BTTN

Packet Design.

In the current BTTN prototype the packet format is simple to keep it short. As shown in Figure 9, the packet consists of pilot-tone, preamble, header, payload, and 1-bit parity. We have described the design of pilot before. The header in the current design contains only two ids for the transmitter and receiver and the [. More will be added in future to implement full-fledged routing functionality. Finally, 32 bit payload delivers the data, and 1 bit parity bit allows for error checking.

3. PROTOTYPING AND EVALUATION OF SINGLE LINK

3.1 Prototype Implementation

The prototype BTTN platform is shown in Figure 10. It is made of 2-layer FR4 PCB in thickness of 31 mils with components on both sides. The PCB was designed using Altium designer software and was manufactured by Goldphoenix Printed Circuit Board Company in Wuhan, China. The antenna is implemented directly on a separate piece of PCB that is attached to the main PCB using SMA connector. This modular design helps future experiments with different types of antennas.

The ADG 904 - SP4T CMOS FET from Analog Devices deployed as the switch [9]; two impedances mentioned in previous section are connected to two input terminal of it. The MCP6561 Low-Power Push-Pull Output Comparator by the Microchip Technologies deployed as the comparator [6]; it links MCU's digital GPIO and envelope detector's output.

The gateway or sink is implemented using a Raspberry PI B+ board [10] taking up the role of the MCU. Here, the comparator output is fed to a GPIO pin of the Raspberry PI that is sampled through Wiring Pi's native C library [20] at the speed of 22MHz [23]. The Raspberry PI communicates with a host computer using the Ethernet via SSH. Thus the whole set up mimics Figure 1.

The exciter (Figure 11(a)) is implemented using a software radio BladeRF [2] and open source software managed by the device provider [3], and modified to fit in our set-up. The BladeRF is connected to a host computer using USB 3.0. In between BladeRF and Laird's 902-928MHz 9dBi circularly polarized antenna [1], we plug RF Bay's 915-LNA series [5] to amplify exciter signal. Whole exciter is mounted on custom designed non RF resistive PVC stand (See Figure 11(b)).

3.2 Evaluation of Single Link using CW Exciter

To evaluate a single link performance in BTTN we carry out a set of experiments with one Tx and one Rx tag and a CW exciter. The goal of these experiments is to measure the maximum achievable link range for different exciter power levels, and demonstrate how we overcome the phase cancellation problem by utilizing two phase channels. All evaluations are done with a single bit rate (5 Kbps) using the exciter generating a CW signals at 915 MHz. The tags are placed in a straight line and the exciter is placed at a position such

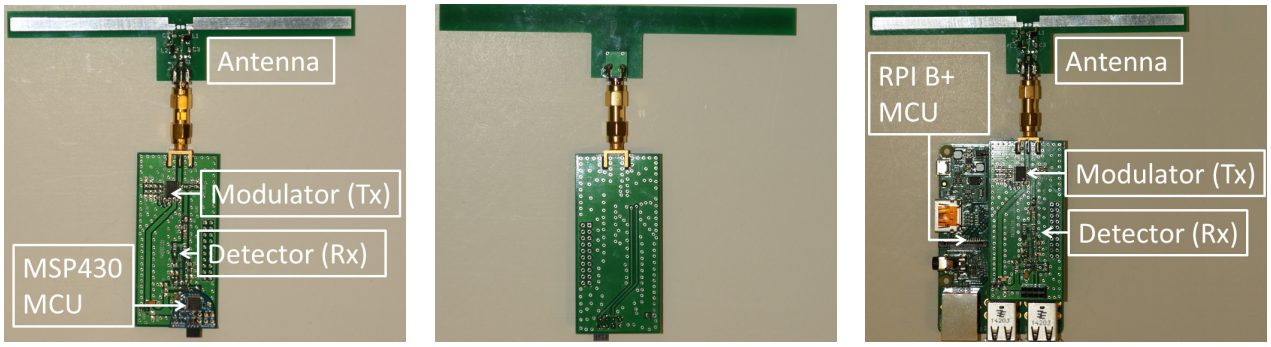

(a) BTTN tag (front) (b) BTTN tag (back) (c) Sink node (Raspberry PI connected to tag)

Figure 10: Various components of the BTTN network: tag and sink.

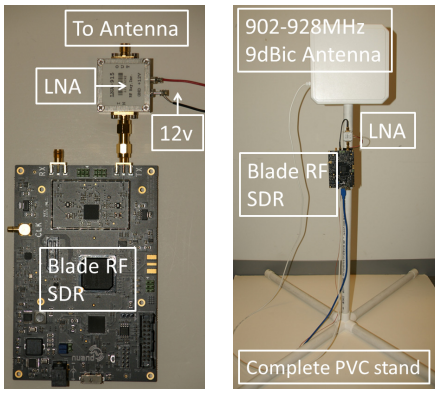

(a) (b)

Figure 11: Exciter set up for BTTN: (a) BladeRF and LNA, (b) entire set up with antenna and PVC stand

that a specified power level is available at Tx tag. The distance between the two tags is varied by moving the Rx tag. Two exciter power levels are used such that the excitation power at the TX tag is about -15 dBm (high power) and -20 dBm (low power) respectively. A simple protocol is used for this evaluation. The Tx tag continuously backscatters a known packet at regular intervals. Each transmission involves a repetition of the same packet over two different phase channels.

Two quantities are measured to characterize the BTTN link performance 1) the amplitude of the baseband signal at the detector output and 2) the bit error rate (BER). The amplitude of the baseband signal at the detector is really the difference between the voltage levels at the envelop detector between the two modulation states denoted by $|V_1 - V_2|$ as depicted in Figure 3. The is the value recorded at the input of the comparator (output of the envelope detector) in the RX tag while the Tx tag backscatters. We use a Texas Instruments A to D converter kit TI-ADS1282EVM-PDK to record these measurements. The detector output is connected to analog input of the kit. The signal is sampled and written to a file on a host computer via the USB port. The BER is evaluated by comparing the bits decoded at the MCU of the RX tag with the known packet being continuously transmitted by the Tx tag. The reported values are based on roughly 10,000 transmitted packets.

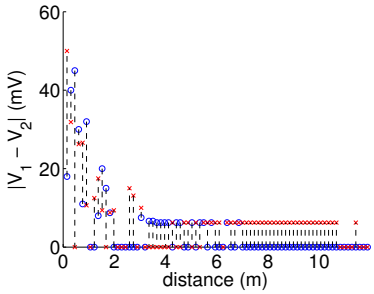

Figure 12: $|V_1 - V2|$ vs distance for the higher power case (-15 dBm) for the two channels shown in different colors. (The black vertical line only serves to pair the corresponding values for two channels.)

Figure 12 shows the $|V_1 - V_2|$ values at different TX-RX distances for the two phase channels for the high power case (-15 dBm). Recall that a larger $|V_1 - V_2|$ (specifically $> \approx 5$mV) is needed for successful decoding. Note the fluctuating patterns for the $|V_1 - V_2|$ for each channel as expected. The somewhat noisy nature of the plot as compared to theoretical prediction in the earlier section (Figure 6) is due to the non-ideal channel behavior (presence of multipath and noise). Also, due to the specific geometry of the setup over a certain range (the three devices being exactly collinear with fixed exciter to Tx distance) the phase cancellation dynamics behaves statically over the range whereby one phase channel always works while these second always fails through the range. This is opposed to an alternating pattern of working channels for other geometries (this is verified analytically by simulating the mathe-

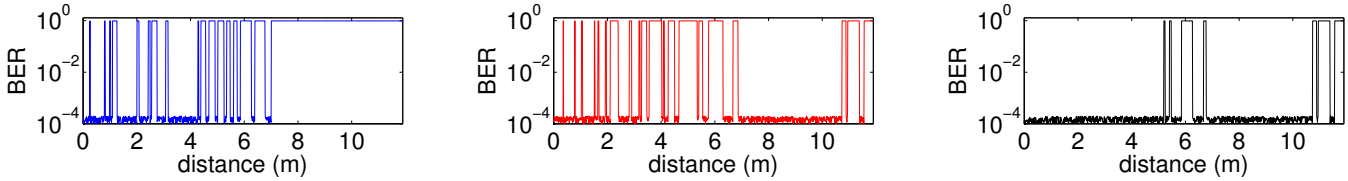

(a) BER on channel 1 (b) BER on channel 2 (c) BER with the best channel

Figure 13: BER vs distance for a single BTTN link with −15 dBm power (higher power) at the backscaterring tag

matical models presented in [31, 22]). Regardless, an important takeway from this plot is the *complementary nature of the two channels*. A lower value for $|V_1 - V_2|$ is one channel is almost always compensated by a higher value in the other channel.

The corresponding BER in each channel (Figure 13) generally tracks $|V_1 - V_2|$ as expected. Below a threshold value (≈5 mV) the BER is very high. With a higher value BER is quite low – in the order of 10^{-4}. Note again the complimentary nature of the two phase channels – when one channel experiences high BER the other one generally acts in a complimentary fashion. Clearly, if the best phase is always chosen at the TX tag, the link provides acceptable performance until about 10 m (Figure 13(c)). The high BER at approx $5 - 7$ m range is likely due to the existence of significant multipath.

Figure 14 shows similar results for the low power case. The plot for of $|V_1 - V_2|$ in this case is nosier because of the lower signal levels. This plot is skipped here for brevity. The noisier nature is apparent also from the shift in the occurrence of high or low BER points when the distance between the tags is varied. However, note again the complimentary behavior of the two phases showing the power of using phase diversity. Once again when the best phase channel is chosen we get a link until about 3 m.

Our results compares favorably with the best reported in literature so far for tag-to-tag links at similar excitation power levels. For example, turbo-charged backscatter [30] reports i) 2.1 m link range at 10 Kbps – 1 Mbps (BER between 10^{-3} and 10^{-4}) with 0 dBm to −20 dBm power, and ii) 9 m link range at 333 bps with −20 dBm power. As explained in Section 2.3 BTTN uses a far less complex technique.

3.3 Phase Cancellation When Using TV Signal as Exciter

The phase cancellation problem and the BTTN approach to address this using phase diversity is not unique to a CW-based exciter. To demonstrate this we also carry out an additional set of experiments using TV signals for excitation. Since our lab receives very poor ambient TV signals (unlike in [26]) we have to resort to artificially producing TV signals. We take the help of the same BladeRF [2] software radio platform paired with a RF Bay's low noise amplifier [5] to produce TV signals in the lab. The gnuradio code developed and manged by device provider [3] is used to generate a 6 MHz ATSC TV signal centered around 915 MHz. We chose this center frequency so as to reuse our hardware prototype without any modifications. The spectrogram is shown in Figure 15. Using a similar arrangement as before we measure the baseband signal amplitude $|V_1 - V_2|$ vs distance. See Figure 16. The plot clearly shows phase cancellation effects and again the complimentary behavior of the two phase channels. This plot is obtained with a different positioning of the exciter and the two tags, now at the corners of a triangle with the exciter in between the tags. This is done specifically to highlight alternating peaks and nulls in each channel with nulls occurring every half wavelength (similar to Figure 6). A somewhat higher power (−15 dBm) is used to reduce the impact of multipath

In this experiment, we do not focus on link range or BER performance. This would require tuning the parameters of the baseband filter and digital decoding implemented in the MCU to account for the larger bandwidth excitation signal. The goal of this experiment is to specifically demonstrate that the phase cancellation does occur irrespective of type of excitation used and that our multiple phase channel method can overcome it. We believe that the authors in [26] did not report cancellations as their link length was small relative to the half wavelength of the ambient TV signals (400 MHz band).

4. MULTIHOP TAG-TO-TAG NETWORK

For multihop operation in BTTN there are two basic issues we need to discuss. The first is the link layer design to avoid interference between neighboring tags. The second is multihop relaying operation.

4.1 Link Layer Design

The BTTN link layer implements a basic listen-before-send mechanism via carrier sensing to avoid interference between neighboring BTTN links. Since the tags have receive ability implementation of carrier sensing is straightforward. The implementation follows the basic ideas outlined in [26]. Before transmission the MCU samples the comparator output to detect presence of

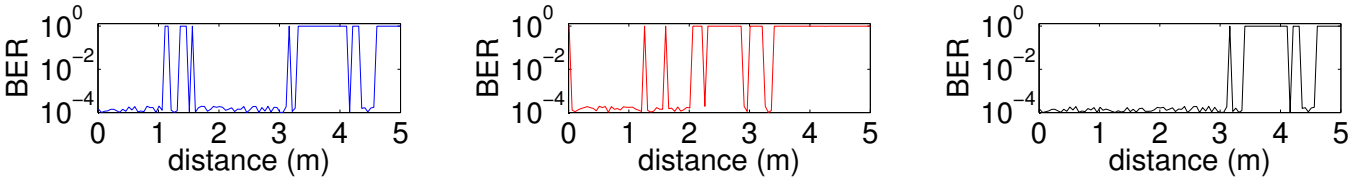

(a) BER on channel 1 (b) BER on channel 2 (c) BER with the best channel

Figure 14: BER vs distance for a single BTTN link with −20 dBm power (lower power) at the backscaterring tag

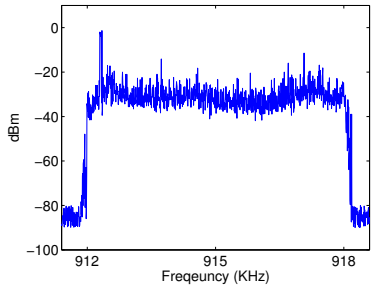

Figure 15: Spectrogram of generated TV signal at 915MHz

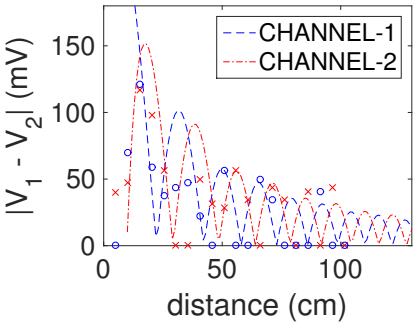

Figure 16: $|V_1 - V_2|$ vs distance with the TV signal as exciter.

pilot tone indicating presence of modulated backscatter. If present, the comparator output flips signifying presence of a neighboring transmission. We also implemented a random backoff strategy mimicking conventional CSMA/CA protocols (e.g., 802.11). The tag backs off for a randomly chosen duration if the carrier is sensed busy. The expected value of this interval doubles for each transmission failure. Each (unicast) transmission is followed by an ack to detect failure.

BTTN tag operates in three distinct modes: *transmit*, *receive* and *listen* modes. By default the tag is always in the listen mode waiting to detect a preamble. Once preamble is detected it switches to the receive mode. In this mode, the tag decodes the packet and after all bits are received checks for correctness using the parity bit. If the packet is correctly received, then it switches to the transmit mode to transmit an acknowledgment. Then, it evaluates the packet header and determines the action to be taken on the packet. For example, it may need to further relay the packet to a neighbor for eventual transmission to the sink node.

The link layer also includes a *learning mechanism* based on probing to learn the best phase channel to use for unicast links between neighboring tags. A probe packet is broadcast in all phase channels (2 in our current design) and all tags receiving the packet respond (unicast) to the broadcasting tag informing which phase channel(s) the probe was correctly received in. The channel information is part of the probe packet. Periodic probing of the neighborhood by all tags ensures that all BTTN links are discovered along with the right transmission parameters. Each tag remembers this information so that the right channel is used to communicate with specific neighbors. For broadcast transmissions, a union of all phase channels must be used. If the union has more than one channel, multiple transmissions of the same packet on multiple channels are needed to cover all neighbors. We evaluated the effectiveness of learning in the sense how many probes are needed to learn the right phase to use. If a large number of probes are needed to learn, then the mechanism is not very efficient. But it turns out that learning is quite robust with just one probe on each phase channel. This is because, for static environments, the link behavior does not exhibit any significant randomness in all experiments we have done. See, e.g., Figure 14 (the BER is either very high or very low).

4.2 Multihop Operation

At this time BTTN tags do not have full-fledged implementation of a multihop routing protocol. This is part of our future work. However, we have evaluated the performance of multihop relaying using a single BTTN tag configured as a transmitter, multiple BTTN tags configured as relays and one BTTN tag configured as the sink. The transmitter continuously transmits a predetermined data packet at regular intervals. The relays listen for a transmission and then backscatter the received data packet. The sink listens and records all received packets. The goal of this experiment is to demonstrate and evaluate the potential of long distance communications via relaying over multiple backscatterring

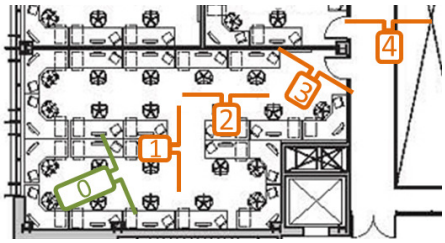

(a) Multihop BTTN set up in lab

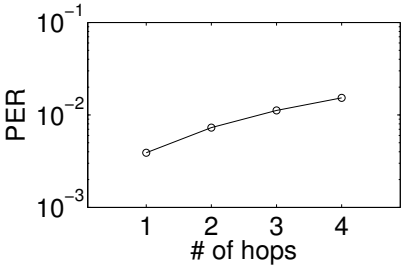

(b) end-to-end multihop PER

Figure 17: Multihop tag-to-tag communication in BTTN over 4 hops (≈12 m).

tags. Once a routing protocol has been implemented, all tags in the BTTN (except the sink) will have the same state machine and will switch between transmit and listen states as specified by the protocol.

The multihop set up extends the scenario we have shown earlier in Section 3 where the excitation power in the environment is set to around −25dBm to −20dBm through the length of the multihop link. We place 5 tags roughly in a line with inter-tag distance roughly about 3 m. One of the tags at the end is also the sink. See Figure 17(a). The set up provides end-to-end distance of about 12 m over 4 hops. The learning mechanism described above is used to learn the best phase to use for each link. 10,000 packets are transmitted from each of the BTTN tags and relayed over $1-4$ hops to reach the sink node. End-to-end packet error rates (PER) are recorded. See Figure 17(b). The packet error rate over 4 hops (total of ≈12 m) is about 1%. This experiment clearly demonstrates the potential of using the BTTN framework for RF-powered passive tags for in-building IoT deployments.

5. RELATED WORK

For more than a decade, the most prominent embodiment of backscatter communication in the research literature has been in RFID technology. Today, standard reader-tag systems are fairly mature and extensively used in practice. More recently, the concept of backscatter-based communication between passive tags has started to gain research interest. Tag-to-tag communication using backscatter between to standard passive tags was explored in [29]. The electromagnetic models that governed this communication were discussed in [27]. These early efforts mostly focused on establishing close-range communication between standard passive tags. In our own prior work, we developed a tag-like radio-less device that had the ability to passively detect communication from a standard RFID tags in its vicinity and communicate with a standard reader using backscattering. We used this device to enable precise localization in of passive RFID tags [13, 11]. While these efforts used an RFID reader to provide the excitation signal for passive tag-to-tag communication, recent efforts have moved away from this to using more general excitation sources. The design presented in [26] use TV signals for the excitation while [24] use WiFi signals for this purpose. In [21], the authors implement advanced MIMO techniques to improve the throughput and range of the tag-to-tag link using TV signals as excitation source. In [18], techniques have been presented to make modulated backscatter emulate signals transmitted by conventional wireless devices like Bluetooth. The techniques that we have developed in this paper address unique challenges that appear in all backscatter based networks including the works mentioned above. In that sense, they can be applied to all such systems to greatly enhance link performance. We also extend a single tag-to-tag link to a multihop network enabling much coverage area for such systems.

6. CONCLUSIONS

Passive backscatter-based tag-to-tag communication holds a tremendous potential in realizing ubiquitous IoT platforms. Based on this paradigm, we have presented the design of a backscattering tag-to-tag network (BTTN) and evaluated its performance. A novel multiphase backscattering technique is presented to overcome a key phase cancellation problem that is inherent to such networks. BTTN implements a learning technique enabling tags to determine the right phase to use for the communication with other tags. We have demonstrated single tag-to-tag link operating reliably at a distance of up to 3 m in the presence of an excitation signal strength of only −20 dBm and at higher distances ($5-10$ m) with more powerful excitation. We have further demonstrated multihop relaying capability of BTTN tags making the network scalable for large area coverage.

While this work has advanced the knowledge of this relatively new communication paradigm, there are several key challenges to enabling the widespread use of these networks. Chief among these are multihop routing protocols and power management strategies. The passive nature of the communication in these networks presents unique problems in these areas. Addressing these issues will be part of our future work.

7. REFERENCES

[1] 902-928 MHZ 9 DBIC CIRCULAR POLARITY PANEL. http://www.lairdtech.com/products/s9028pcl-s9028pcr.

[2] bladeRF - the USB 3.0 Superspeed Software Defined Radio. http://nuand.com/.

[3] bladeRF USB 3.0 Superspeed Software Defined Radio Source Code. https://nuand.com/forums/.

[4] HSMS-285x Series: Surface Mount Zero Bias Schottky Detector Diodes. http://www.avagotech.com/docs/AV02-1377EN.

[5] LNA Series 902-928MHz Low Noise Amplifier. http://rfbayinc.com/products_pdf/product_75.pdf.

[6] MCP6561, 1.8V Low-Power Push-Pull Output Comparator. http://www.microchip.com/downloads/en/DeviceDoc/22139C.pdf.

[7] Texas Instruments MSP430 family of ultra-low-power microcontrollers. http://www.ti.com/lit/ds/slas491i/slas491i.pdf.

[8] UHF Gen2 Air Interface Protocol. http://www.gs1.org/epcrfid/epc-rfid-uhf-air-interface-protocol/2-0-1.

[9] Wideband 2.5 GHz, 37 dB Isolation at 1 GHz, CMOS 1.65 V to 2.75 V, 4:1 Mux/SP4T. http://www.analog.com/media/en/technical-documentation/data-sheets/ADG904_904R.pdf.

[10] RASPBERRY PI 1 MODEL B+. https://www.raspberrypi.org/products/model-b-plus/, 2014.

[11] Akshay Athalve and Petar M Djuric. RFID system and method for localizing and tracking a moving object with an RFID tag. US Patent 7,812,719.

[12] A. Athalye, V. Savic, M. Bolic, and P.M. Djuric. A radio frequency identification system for accurate indoor localization. In *IEEE Proc. of ICASSP*, May 2011.

[13] Akshay Athalye, Vladimir Savic, Miodrag Bolic, and Petar M Djuric. Novel semi-passive RFID system for indoor localization. *Sensors Journal, IEEE*, 13(2):528–537, 2013.

[14] Luca Bedogni, Marco Di Felice, Fabio Malabocchia, and Luciano Bononi. Indoor communication over TV gray spaces based on spectrum measurements. In *Wireless Communications and Networking Conference (WCNC), 2014 IEEE*, pages 3218–3223. IEEE, 2014.

[15] Dinesh Bharadia, Kiran Raj Joshi, Manikanta Kotaru, and Sachin Katti. Backfi: High throughput wifi backscatter. In *Proceedings of the 2015 ACM Conference on Special Interest Group on Data Communication*, SIGCOMM '15, pages 283–296. ACM.

[16] Ayon Chakraborty and Samir R. Das. Measurement-augmented spectrum databases for white space spectrum. In *Proceedings of the 10th ACM International on Conference on Emerging Networking Experiments and Technologies*, CoNEXT '14, pages 67–74. ACM.

[17] D. M. Dobkin. *The RF in RFID: Passive UHF RFID in Practice*. Elsevier - Newnes, 2007.

[18] J.F. Ensworth and M.S. Reynolds. Every smart phone is a backscatter reader: Modulated backscatter compatibility with bluetooth 4.0 low energy (ble) devices. In *RFID (RFID), 2015 IEEE International Conference on*, pages 78–85, April 2015.

[19] K. Finkenzeller. *RFID Handbook*. Wiley, third edition, 2010.

[20] Gordon Henderson. Wiring Pi, GPIO Interface library for the Raspberry Pi. http://wiringpi.com/.

[21] Pan Hu, Pengyu Zhang, and Deepak Ganesan. Laissez-faire: Fully asymmetric backscatter communication. In *Proceedings of the 2015 ACM Conference on Special Interest Group on Data Communication*, SIGCOMM '15, pages 255–267. ACM.

[22] Jinghui Jian. EM field analysis for phase cancellation in backscattering tag to tag systems, 2015. Available at http://wings.cs.sunysb.edu/bttn/techreport2.pdf.

[23] Joonas Pihlajamaa. Benchmarking Raspberry Pi GPIO Speed. http://codeandlife.com/2012/07/03/benchmarking-raspberry-pi-gpio-speed/.

[24] Bryce Kellogg, Aaron Parks, Shyamnath Gollakota, Joshua R Smith, and David Wetherall. Wi-fi backscatter: internet connectivity for RF-powered devices. In *Proceedings of the 2014 ACM Conference on Special Interest Group on Data Communication*, SIGCOMM '14, pages 607–618. ACM.

[25] K. Kurokawa. Power waves and the scattering matrix. *Microwave Theory and Techniques, IEEE Transactions on*, 13(2):194–202, Mar 1965.

[26] Vincent Liu, Aaron Parks, Vamsi Talla, Shyamnath Gollakota, David Wetherall, and Joshua R. Smith. Ambient backscatter: Wireless communication out of thin air. In *Proceedings of the 2013 ACM Conference on Special Interest Group on Data Communication*, SIGCOMM '13, pages 39–50.

[27] G. Marrocco and S. Caizzone. Electromagnetic models for passive tag-to-tag communications.

Antennas and Propagation, IEEE Transactions on, 60(11):5381–5389, Nov 2012.

[28] Pavel V Nikitin, KV Seshagiri Rao, Sander F Lam, Vijay Pillai, Rene Martinez, and Harley Heinrich. Power reflection coefficient analysis for complex impedances in rfid tag design. *IEEE Transactions on Microwave Theory and Techniques*, 53(9):2721–2725, 2005.

[29] P.V. Nikitin, S. Ramamurthy, R. Martinez, and K.V.S. Rao. Passive tag-to-tag communication. In *RFID (RFID), 2012 IEEE International Conference on*, pages 177 –184, april 2012.

[30] Aaron N Parks, Angli Liu, Shyamnath Gollakota, and Joshua R Smith. Turbocharging ambient backscatter communication. In *Proceedings of the 2014 ACM Conference on Special Interest Group on Data Communication*, SIGCOMM '14, pages 619–630.

[31] Zhe Shen, Akshay Athalye, and Petar M. Djurić. Phase cancellation in backscastter based tag-to-tag communication systems, To Appear. Draft available at http://wings.cs.sunysb.edu/bttn/techreport1.pdf.

[32] S. Thomas and M.S. Reynolds. QAM backscatter for passive UHF RFID tags. In *RFID, 2010 IEEE International Conference on*, pages 210–214. IEEE, 2010.

[33] Jing Wang and M. Bolic. Exploiting dual-antenna diversity for phase cancellation in augmented RFID system. In *Smart Communications in Network Technologies (SaCoNeT), 2014 International Conference on*, pages 1–6.

[34] Tan Zhang, Ning Leng, and Suman Banerjee. A vehicle-based measurement framework for enhancing whitespace spectrum databases. In *Proceedings of the 20th annual international conference on Mobile computing and networking*, MOBICOM '14, pages 17–28. ACM.